# Single-cell transcriptomics identifies aberrant glomerular angiogenic signalling in the early stages of WT1 kidney disease

JC Chandler *et al. J Pathol* https://doi.org/10.1002/path.6339

**Supplementary materials and methods**

**Supplementary Figures S1–S4**

**Supplementary Tables S1, S2 are provided as separate Excel files**

**Supplementary Table S3**

Reference numbers refer to the main text list

## Supplementary materials and methods

### *Human tissue*

Human tissue was sourced from Great Ormond Street Hospital for Children NHS Foundation Trust, UK, from patients with *WT1* pathogenic variants and who received treatment after 2012, under the remit of the IMPORT/UMBRELLA study, for which we hold ethical approval (London Bridge REC 12/LO/0101, IRAS: 62637) or for those who were not registered under the IMPORT/UMBRELLA study, under the remit of the CCLG tissue bank ethics. Both patients were diagnosed with Denys–Drash syndrome (DDS), defined as having Wilms' tumour, nephropathy presenting as persistent proteinuria or overt nephrotic syndrome, and genitourinary anomalies (MIM#194080): the first was male (*WT1 c.1214A>G*; p.His405Arg) [46,59] and the second was female (*WT1 c.1180C>T*; p.Arg394Trp) with histologically defined diffuse mesangial sclerosis [46]. Three paediatric control samples were also provided. Additional tissue was sourced from the Hôpital Universitaire Necker-Enfants Malades, France from the Imagine Biocollection under ethics approved by French Minister of Research (DC-2020-3994) and the French Ethics Committee for Research (IRB registration number #00011928) from a female patient with

haemolytic uremic syndrome and DDS (*WT1* c.*1097G>A*; p.Arg366His), with histologically defined thrombotic microangiopathy [45]. One paediatric control sample was also provided.

### *Histological and biochemical assessment of experimental animals*

Frozen mouse sperm from C57BL/6 male mice, heterozygous for *Wt1 c.1800 C>T* p. R394W (*Wt1*$^{R394W/+}$), courtesy of V. Huff, MD Anderson Cancer Centre, were used to implant C57BL/6 females. Litters were crossed with C57BL/6 mice and genotyped as previously described [11]. Male heterozygous C57BL/6 mice were then backcrossed with MF1 females (Charles River, Margate, UK) for two generations [11]; second-generation male offspring (*Wt1*$^{R394W/+}$) were used for all subsequent analyses. All procedures were approved by the UK Home Office. Renal function was assessed at 4, 8 and 10 weeks of age by urinary albumin/creatinine ratio (ACR) via enzyme-linked immunosorbent assay of albumin (Bethyl Laboratories, Montgomery, TX, USA) and creatinine (500701, Cayman Chemical, Ann Arbor, MI, USA). Blood urea nitrogen (BUN) levels were quantified in plasma taken at 4 and 8 weeks of age using the QuantiChrom$^{TM}$ Urea Assay Kit (DIUR-100, BioAssay Systems, Hayward, USA). Plasma pro-adrenomedullin (pro-AM) levels were analysed via ELISA (orb775953, Biorbyt, Cambridge, UK). Histological analyses were conducted on 7-µm sections stained with Periodic Acid–Schiff.

### *Glomerular isolation and preparation of single cell suspensions*

Due to the smaller size of mice at 4 weeks old, limiting the efficacy of inter-arterial bead perfusion, transcardial perfusion was used to increase glomerular yield, mice were perfused with 40 ml of ice-cold Hanks' Balanced Salt Solution without calcium and magnesium (HBSS$^{-/-}$), containing 300 µl M-450 Epoxy Dynabeads (14011, Invitrogen, Waltham, USA). Both kidneys were removed and minced into small pieces with a scalpel and incubated in 3 ml prewarmed digestion buffer (1.5 U/ml Liberase TM, 100 U/ml DNase I in HBSS$^{-/-}$) at 37°C for 20 min with constant agitation (300 RPM) in a ThermoMixer (Eppendorf, Hamburg, Germany). All subsequent steps were

performed as previously described [8,14], with the addition of bovine serum albumin (BSA)-coated plastics throughout to prevent cell adhesion (10% BSA in $DPBS^{-/-}$ and rinsed with $DPBS^{-/-}$).To enhance podocyte number in the final cell fraction, the mechanical digest approach was optimised as follows: gentle pipetting every 10 min for 30 min, after 30 min each sample was transferred into a 2 ml syringe (without passing via the needle) and slowly and steadily pushed through a 25½ gauge needle followed by a 27½ gauge needle (smaller gauge needles were not used as these were associated with podocyte loss). Samples were then incubated for an additional 5 minutes with one pipette mix. At 45 min the digest was 'stopped' with 10 ml ice-cold $DBPS^{-/-}$ with 10% foetal bovine serum (FBS) and placed on a magnetic separator to remove magnetic beads. The supernatant was sieved (100-µm cell strainer) and rinsed with $DPBS^{-/-}$ + 10% FBS to remove aggregates. Cells were resuspended in $DPBS^{-/-}$ + 2% FBS, 5 mM EDTA and underwent a live/dead cell sort with propidium iodide viability dye with 98.1–98.9% viability across all four samples.

***Library preparation, single-cell sequencing and alignment***

GEMs underwent 3' GEX library preparation and libraries were pooled. All four samples underwent 150 base pair (bp) paired-end read sequencing on one lane of an S4 flow cell (Illumina NovaSeq 6000) to a minimum depth of 500 million reads per sample (Source BioScience, Nottingham, UK). Reads were mapped individually from each sample to the 10x-approved gex-mm10-2020-A mouse reference sequence using 10X Genomics Cell Ranger v5.0.1 [78]. Data were separately aligned to the *Wt1* primary transcript using HISAT2 v2.2.1 [79] to confirm the presence of the Wt1p.R394W heterozygous mutation in the two $Wt1^{R394W/+}$ samples.

***Quality control and pre-processing of single-cell sequencing data***

Single-cell sequencing data were aggregated and processed using Seurat (v4.1.1) [80] in R Studio (v 2022.02.0). The full script for analysis had been made available at https://github.com/daniyal-jafree1995/collaborations/blob/main/Chandleretal_2022_WT1glomerulopathyscRNAseq.

Quality control criteria were empirically determined, including the removal of cells with fewer than 150 RNA features or mitochondrial feature representation greater than 20% and putative doublets (DoubletFinder 2.0.3 [81]). 93.77% of cells (6846/7301) were retained in the final count matrix, with levels consistent across each donor. The resulting count matrix was corrected for ambient RNA contamination using the SoupX (v1.6.1) package [82]. Samples were then normalised, scaling expression by all genes detected, before dimension reduction with principal component analysis, which identified 16 informative principal components. This reduced dataset was used for nearest-neighbour graph construction and unsupervised clustering (Louvain method), with a 0.4 resolution selected based on apparent cluster separation on indicative marker genes and visualised by UMAP.

***Cell-type identification***

Cell-type cluster canonical markers were visualised using the DotPlot function in Seurat and included *Wt1* and *Nphs2* for podocytes, *Emcn* and *Ehd3* for glomerular endothelial cells, *Ptn* and *Pdgfrb* for mesangial cells, *Sox17* for arterial subsets including *Plvap*-expressing efferent arteriole and *Edn1*-expressed afferent arteriole, *Acta2* and *Myh11* for vascular smooth muscle cells, *Pax8* and *Cldn1* for parietal epithelial cells, *Ptprc* (*Cd45*) labelling all immune cells and *Lyz2, Cd79a* and *Igkc* or *Cd3e* and *Trbc2* to discriminate myeloid, B-cell and T-cell lineages, respectively. Cell-type proportions were visualised using bar graphs in Prism (v9.3.1, GraphPad Software, Boston, MA, USA).

***Differential expression and gene ontology analysis***

The FindMarkers function (using the Wilcoxon Rank Sum test) in Seurat was used to perform cell-specific differential expression analysis between wildtype and mutant cells, defining a differentially expressed gene as one with an average $\log_2$ fold change (FC) > 0.25 and adjusted *p* value < 0.05. Results of differential expression were visualised using heatmaps or violin plots in Seurat and EnhancedVolcano (v1.12.0) plots. WT1 motif analysis was done using CiiiDER, within 1k base-pairs downstream and 500 base-pairs upstream of the transcriptional start site [5], with stringency set to 0.1 and the WT1 motif (MA1627.1) defined by JASPAR 2022. Gene ontology (GO) analysis was performed by manually exporting lists of differentially expressed genes into the PANTHER webtool to group genes into GO biological processes [83]. Statistical overrepresentation (Fisher's exact test) was performed to calculate an enrichment score and false discovery rate for each GO term, before plotting results in Prism.

***Ligand-receptor pair analysis***

Inference of glomerular intercellular communication was performed using the NICHES package [18]. NICHES calculates the product of ligand expression by a given cell and the expression of its putative receptors in a pairwise manner, thus providing ligand-receptor analysis single-cell resolution. A NICHES object was created from a subset of the annotated scRNA-seq dataset containing only cells within the glomerular tuft, including podocytes and their physical or paracrine signalling candidates: glomerular endothelial cells, mesangial cells and parietal epithelial cells. The dataset was partitioned by genotype, before imputing ligand-receptor pairs for $Wt1^{+/+}$ or $Wt1^{R394W/+}$ glomerular cell-types. A NICHES UMAP was created to visualise the pairwise interactions in two-dimensional space and the OmniPath database [84] was used to create a list of putative ligand-receptor interactions between each cell pair. This list of putative ligand-receptor pairs was then manually curated, first by validating interactions on STRING [85] (with 'Co-occurrence' and 'Text-mining' excluded to ensure interactions came from curated databases/experimental data only), followed by mining of the literature, to only include established intercellular interactions. The curated lists were used to generate heatmaps, where

the average $log_2$FC is presented, listed in order of adjusted *p* value and grouped by enrichment in *Wt1*$^{+/+}$ glomeruli or *Wt1*$^{R394W/+}$ glomeruli or those that were conserved across both.

### *Cross-disease comparison of podocyte differential gene expression*

To compare podocytes in *Wt1*$^{R394W/+}$ glomerulopathy with other models of early glomerular disease, publicly accessible scRNA-seq data from Dynabead isolated glomeruli were used [8]. These included a nephrotoxic nephritis model (NTN, *n* = 2 mice and *n* = 2 controls) harvested at 5 days post injection in the absence of glomerulosclerosis. The second dataset was a leptin-deficiency (BTBR *Lep*$^{ob/ob}$, *n* = 2 mutants and *n* = 2 controls) model of type 2 diabetes, taken at 12 weeks of age, characterised by proteinuria prior to glomerular lesions. The final dataset was a model of congenital nephrotic syndrome due to *Cd2ap* deficiency (*Cd2ap*$^{-/-}$, *n* = 1 mouse or without *Cd2ap*$^{+/+}$, *n* = 1 mouse) taken at 3 weeks, soon after the onset of proteinuria. Count matrices for each disease and their respective control groups were downloaded from the National Center for Biotechnology Information Gene Expression Omnibus (GSE146912). The quality control and pre-processing steps described above were applied separately to each dataset, to account for differences in data quality, batch effects and experimental conditions, such as murine genetic background. For each dataset, a further processing step of batch integration was performed using the Harmony package [86] to ensure clustering of diseased and healthy podocytes within each condition. Podocytes were then identified by the co-expression of *Nphs1* and *Nphs2*. Differential expression analysis was run for healthy and diseased podocytes independently for each dataset, as above, and the resulting lists were manually compared with that of *Wt1*$^{R394W/+}$ glomerulopathy. The full script for the cross-disease comparison of scRNA-seq data has been made publicly available: https://github.com/daniyal-jafree1995/collaborations/blob/main/Chandleretal_2022_crossglomdiseasecomparison.R. The number of differentially expressed genes present in each pathology were used to construct Venn diagrams. The upregulation or downregulation of genes was conserved by podocytes across all pathologies and those unique to *Wt1*$^{R394W/+}$ glomerulopathy were used to construct heatmaps.

Each of the 23 conserved upregulated and five downregulated genes (found in all four analysed murine scRNA-seq datasets) then underwent targeted screening for similar dysregulation (fold-change > 0.25 and $p < 0.05$) in the Nephroseq database nephroseq.org of human microarray data, restricted to glomerular datasets only.

### *Primary podocyte harvest and culture*

For primary podocyte harvest, glomeruli were isolated from *Wt1*$^{+/+}$ and *Wt1*$^{R394W/+}$ mice at 4 weeks of age. In brief, kidneys were digested in DPBS$^{-/-}$ with 1 mg/ml Collagenase A (C2674, Sigma) and 200 U/ml DNASe I (18047-019, Invitrogen) for 30 min at 37°C with gentle agitation. Collagenase digested tissue was then sieved through a 100-µm cell strainer, collected by centrifugation and resuspended in 1 ml DPBS$^{-/-}$. After washing, glomeruli were resuspended in growth medium [RPMI-1640 (21875091, ThermoFisher, Waltham, USA) with 10% FBS, 1% Penicillin-Streptomycin stock solution and 1% Insulin-Transferrin-Selenium stock solution (41400045, ThermoFisher)] and plated on Matrigel (354234, Corning, Flintshire, UK) coated plates. Glomeruli were incubated at 37°C, in 5% $CO_2$ for 7 days, at which point glomeruli were removed by 30-µm sieving and podocytes were left to fully differentiate for another 3 days.

### *Immunofluorescence*

Immunofluorescence staining on murine tissue was performed on 7-µm cryosections using primary antibodies against WT1 (1:100, ab89901, Abcam, Cambridge, UK), F4/80 (MCA497G, Bio-Rad, Watford, UK) and CD31 (1:400, MA3105, ThermoFisher) and imaged on a Zeiss Observer 7 Colour Fluorescence with Hamamatsu Flash 4.0v3 camera. The number of WT1$^+$ cells found within the glomerular tuft was counted in 50 glomeruli per section and averaged for each individual mouse. CD31$^+$ staining was quantified as percentage coverage of tuft area in 50 glomeruli per section calculated in FIJI [19] and averaged per animal. For myeloid counts, F4/80$^+$ cells were counted within the glomerulus and in the field of vision outside the glomerulus at a

consistent magnification, counts were taken over 50 glomeruli per animal and averaged for each mouse. For human tissue, immunofluorescence staining for CD31 (1: 200, ab76533, Abcam) was performed on 7-µm wax sections, with every available glomerulus in the biopsy imaged and analysed, as previously described.

### *Tube formation assay*

Primary podocytes isolated from *Wt1*$^{+/+}$ and *Wt1*$^{R394W/+}$ mice at 4 weeks of age were seeded at a density of 150,000 cells/well in a 6-well plate, in 1 ml of RPMI media with 5% FBS (RPMI + 5% FBS) and left for 48 h. The conditioned media was then used for glomerular endothelial angiogenesis assays. For this, 12,000 primary murine glomerular endothelial cells (C57-6014G, Cell Biologics, Chicago, USA) were seeded into µ-Slide 15 Well 3D (81506, Ibidi, Gräfelfing, Germany), onto growth-factor reduced Matrigel® (734-0268, VWR, Lutterworth, UK), suspended in each conditioned media, or RPMI + 5% FBS; each condition was run in triplicate and cells were between passages 4 and 6. Cells were imaged on an EVOS M5000 (Thermo Fisher Scientific) at 0 h to determine cell seeding density to be within ±10% and at 6 h, for final tube formation quantified using FastTrack AI (MetaVi Labs, Austin, USA), as previously described [87]. Experiments were conducted on three independent occasions and the average is presented. To investigate a role for adrenomedullin in glomerular endothelial angiogenesis, secreted pro-adrenomedullin levels were quantified via ELISA (orb775953, Biorbyt) in media conditioned by *Wt1*$^{R394W/+}$ podocytes and correlated with the associated glomerular endothelial cell angiogenic parameters. *Wt1*$^{R394W/+}$ conditioned medias were then spiked with 200 nM of rat adrenomedullin (A3830, Merck, Gillingham, UK) and used for subsequent glomerular endothelial angiogenesis analyses as described.

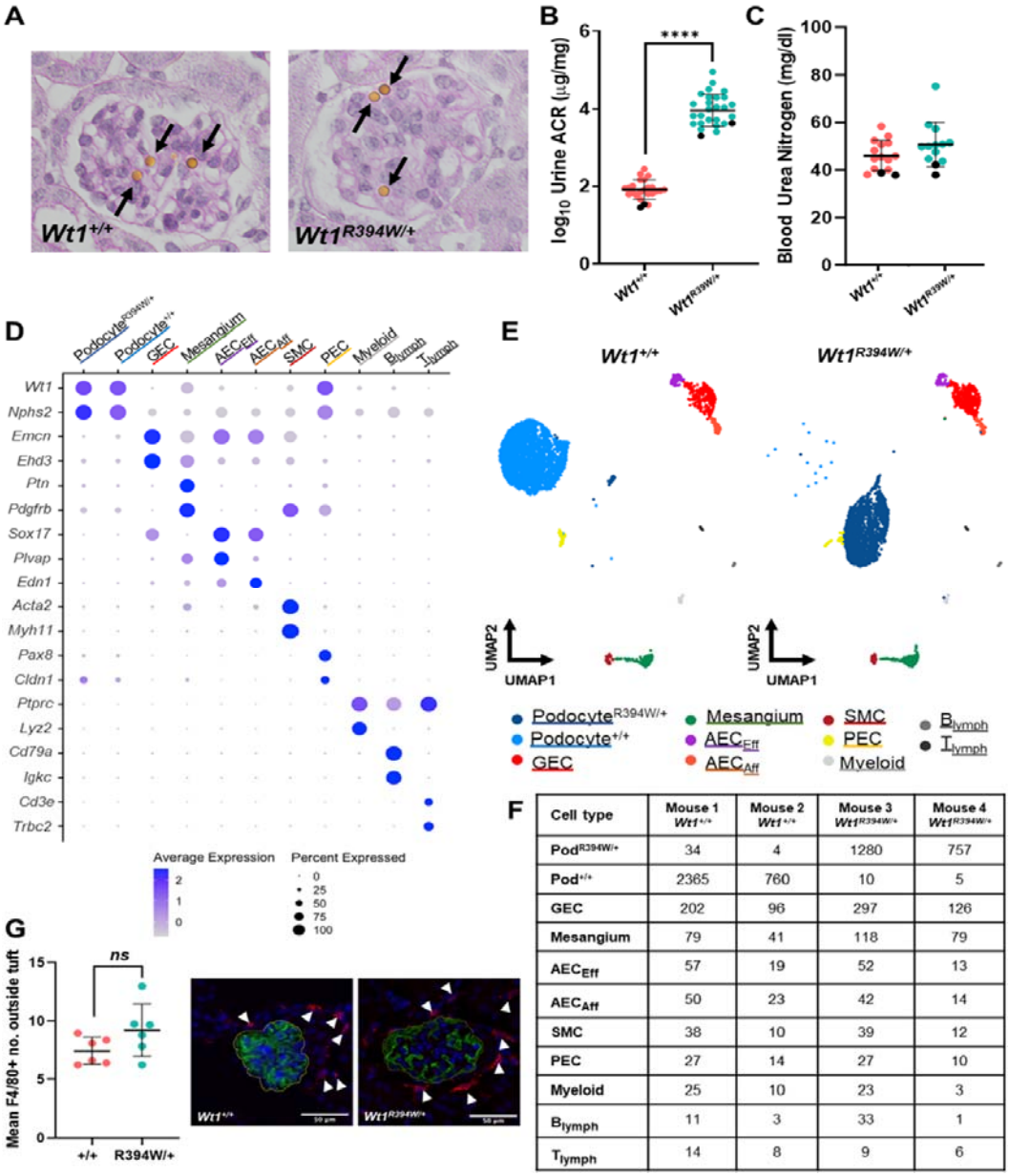


| Cell type | Mouse 1 *Wt1*+/+ | Mouse 2 *Wt1*+/+ | Mouse 3 *Wt1*R394W/+ | Mouse 4 *Wt1*R394W/+ |
|---|---|---|---|---|
| Pod$^{R394W/+}$ | 34 | 4 | 1280 | 757 |
| Pod$^{+/+}$ | 2365 | 760 | 10 | 5 |
| GEC | 202 | 96 | 297 | 126 |
| Mesangium | 79 | 41 | 118 | 79 |
| $AEC_{Eff}$ | 57 | 19 | 52 | 13 |
| $AEC_{Aff}$ | 50 | 23 | 42 | 14 |
| SMC | 38 | 10 | 39 | 12 |
| PEC | 27 | 14 | 27 | 10 |
| Myeloid | 25 | 10 | 23 | 3 |
| $B_{lymph}$ | 11 | 3 | 33 | 1 |
| $T_{lymph}$ | 14 | 8 | 9 | 6 |

## Supplementary Figures S1–S4

**Figure S1. Supporting data for single-cell RNA seq analyses.** (A) Glomeruli from *Wt1*$^{+/+}$ and *Wt1*$^{R394W/+}$ mice after Dynabead perfusion confirming bead penetration into *Wt1*$^{R394W/+}$ glomeruli at 4 weeks of age, prior to advanced glomerulosclerosis, confirming a non-biased harvest. (B) $Log_{10}$ albumin:creatinine ratio (ACR) at 4 weeks of age with scRNA-seq donors highlighted in black, demonstrating their representative nature of the *Wt1*$^{R394W/+}$ mouse line. (C) Blood urea nitrogen (BUN) levels at 4 weeks of age with scRNA-seq donors highlighted in black, demonstrating their representative nature. (D) Dot blot of canonical marker genes used for cluster resolution for 11 cell type clusters. (E) UMAPs split by *Wt1*$^{+/+}$ and *Wt1*$^{R394W/+}$ genotype, showing clear representation from both genotypes in each cell type cluster, with the exception of podocytes. (F) Table of cell counts by cell type cluster and mouse donor, showing contribution from all four mice to each cluster, with the exception of podocytes. (G) Extraglomerular myeloid (F4/80+) cell counts, present in the area outside if the glomerular tuft in 4-week-old glomeruli (averaged over 50 glomeruli per animal) show no significant difference between *Wt1*$^{+/+}$ (7.48±0.48) and *Wt1*$^{R394W/+}$ (9.21±0.92) mice (*t*-test; $p = 0.1200$, $n = 6$ mice per group). Scale bars:

50 μm. AEC, arterial endothelial cell; GEC, glomerular endothelial cell; PEC, parietal epithelial cell; SMC, smooth muscle cell.

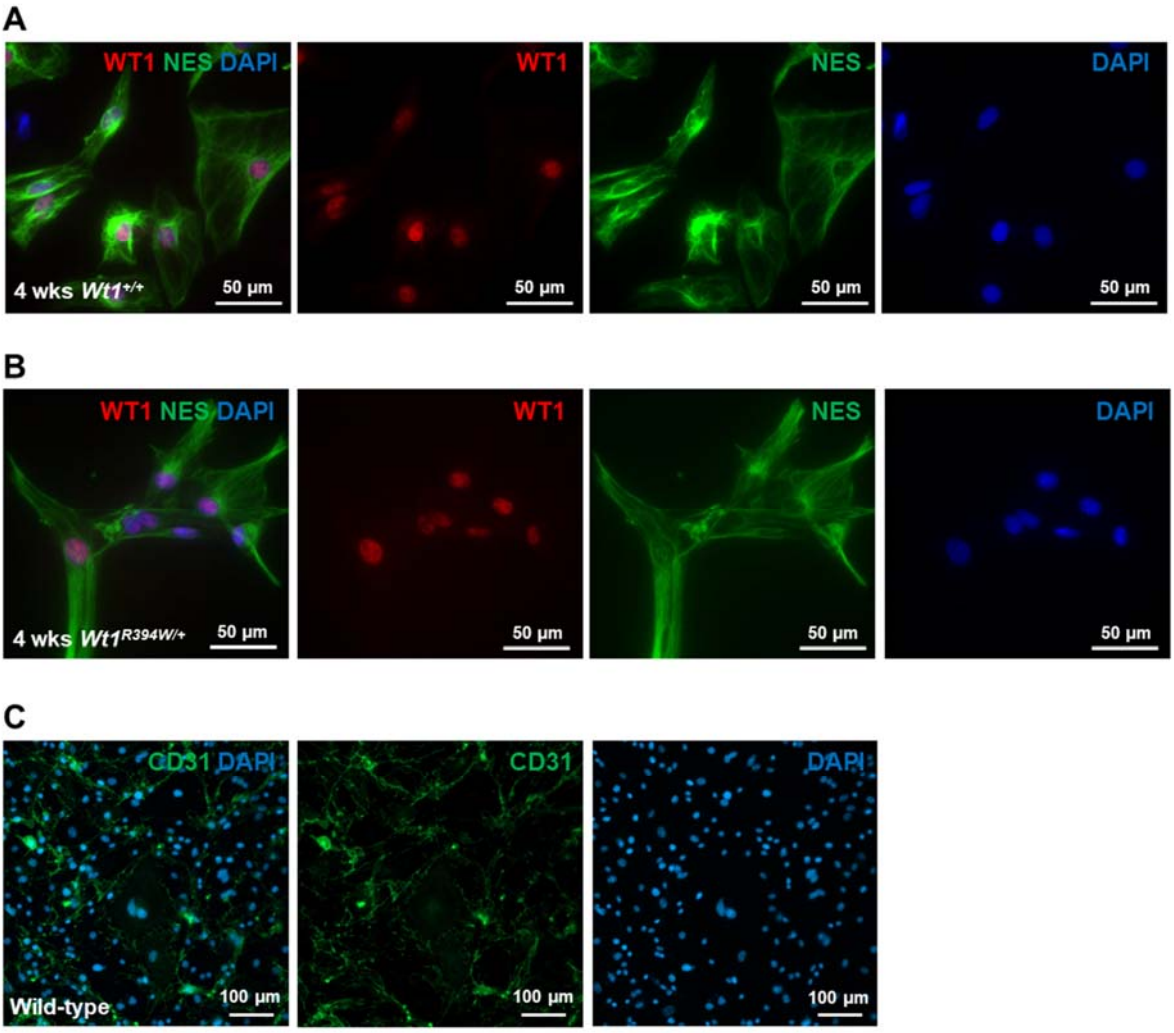


**Figure S2**. **Characterisation of primary cell lines.** (A,B) Primary podocytes isolated from (A) *Wt1*$^{+/+}$ and (B) *Wt1*$^{R394W/+}$ mice at 4 weeks of age show positive staining for the canonical markers Wilms tumour 1 (WT1) and Nestin (NES), with a DAPI nuclear stain. Scale bars: 50 µm. (C) Primary wild-type mouse glomerular endothelial cells (GECs) show positive staining for cluster of differentiation 31 (CD31). Scale bars: 100 µm.

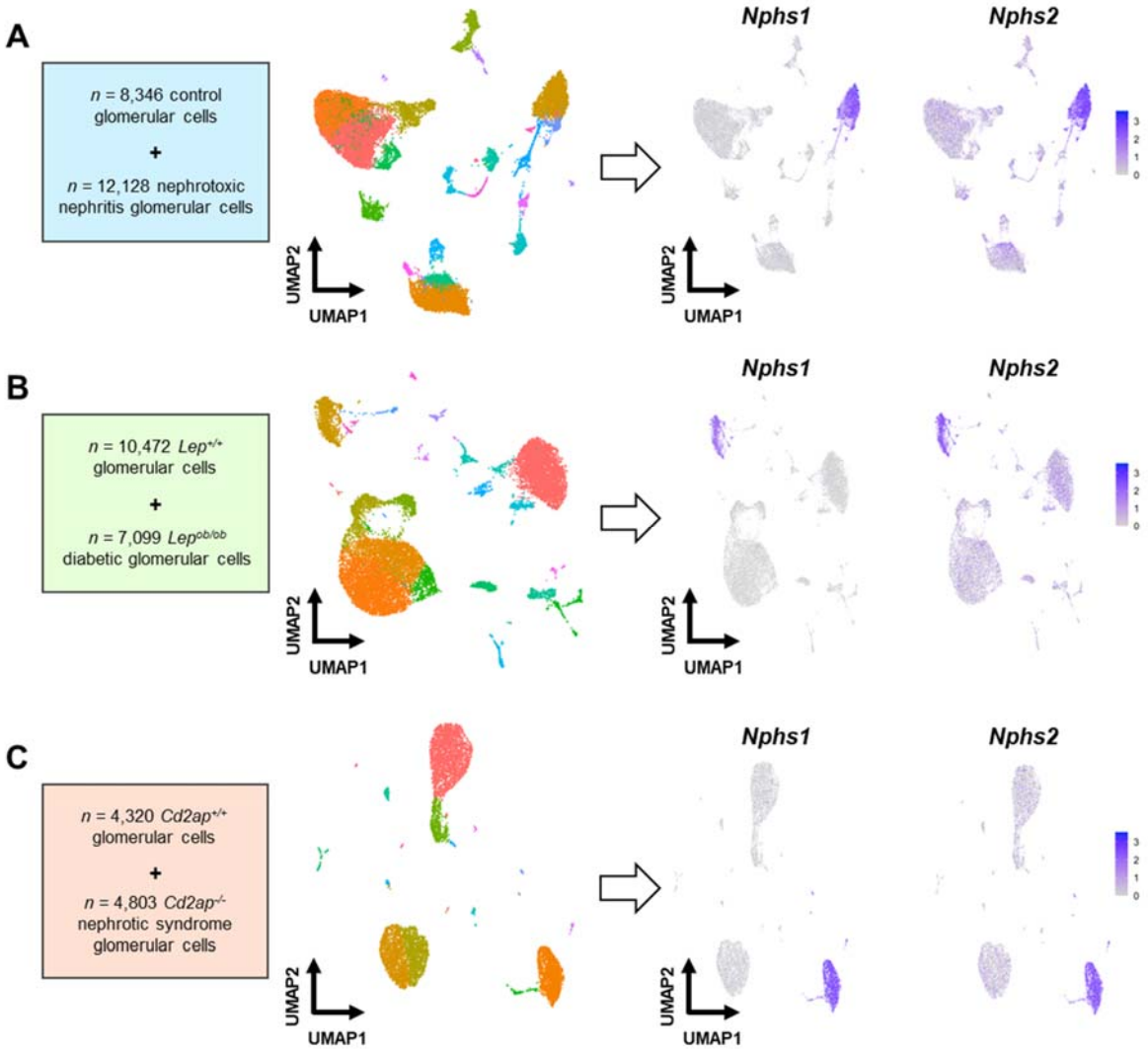


**Figure S3. Isolation of podocytes from scRNA-seq data from additional murine models of glomerular disease for cross-disease comparison**. Data were derived from the National Center for Biotechnology Information Gene Expression Omnibus (GSE1469129) and included: (A) Two mice 5 days after induction with nephrotoxic nephritis (NTN, *n* = 1,450 podocytes) and two control mice (*n* = 1,491 podocytes). (B) Two 12-week-old mice carrying a leptin mutation in homozygosity *(Lep*$^{ob/ob}$, *n* = 713 podocytes) modelling diabetic nephropathy and two littermate controls (*Lep*$^{+/+}$, *n* = 869 podocytes). (C) One *Cd2ap*$^{-/-}$ mouse with congenital nephrotic syndrome (*n* = 423 podocytes) and one littermate control (*n* = 1,337 podocytes). UMAPs were generated from each dataset independently and podocytes were identified by co-expression of *Nphs1*+ and *Nphs2*+. Differential expression analysis between healthy and diseased podocytes within each dataset served as an input for cross-disease comparison with the *Wt1*$^{R394W/+}$ model.

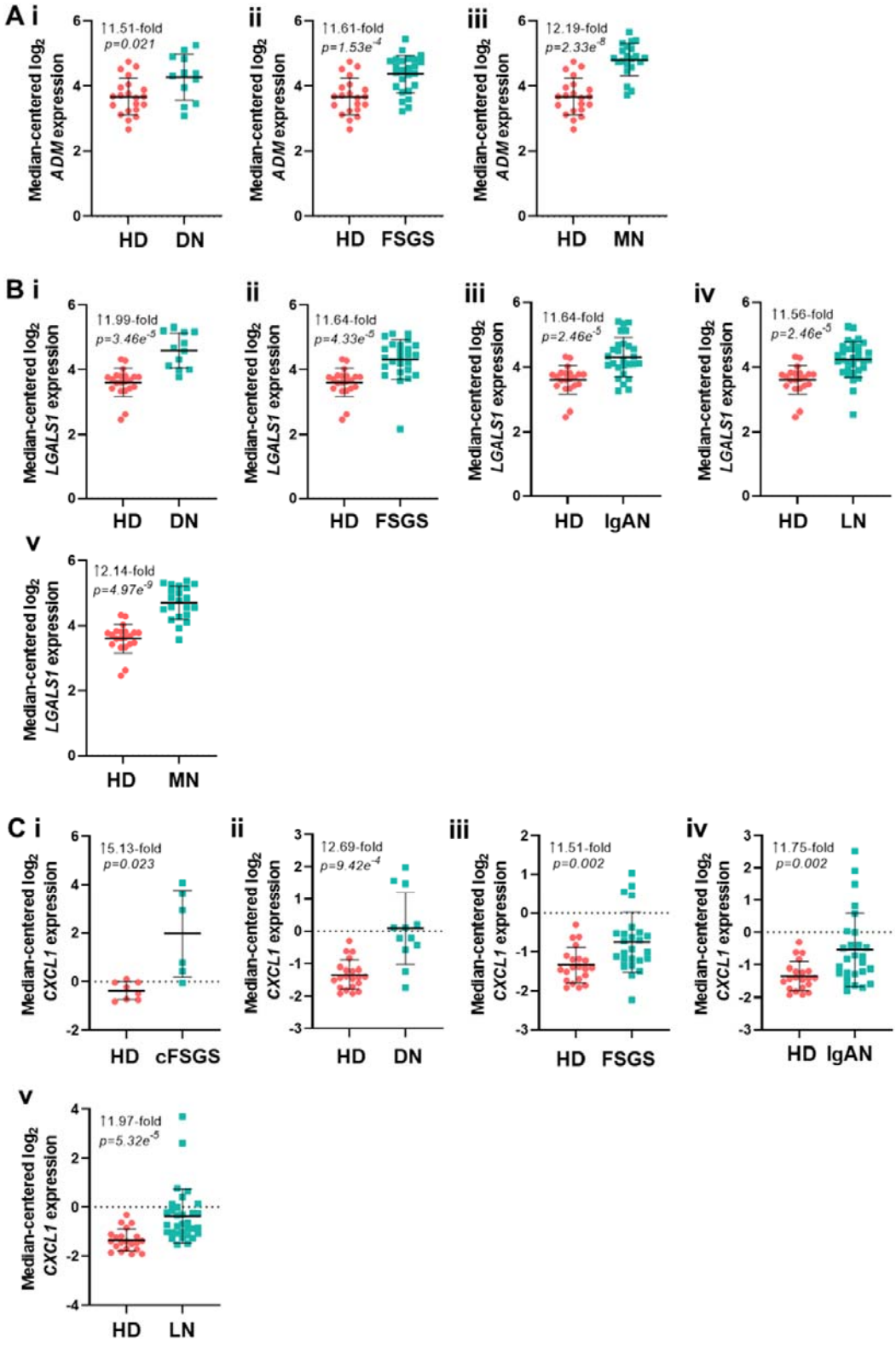
A i
↑1.51-fold
p=0.021
Median-centered log2 ADM expression
HD DN
ii
↑1.61-fold
p=1.53e-4
HD FSGS
iii
↑2.19-fold
p=2.33e-8
HD MN
B i
↑1.99-fold
p=3.46e-5
Median-centered log2 LGALS1 expression
HD DN
ii
↑1.64-fold
p=4.33e-5
HD FSGS
iii
↑1.64-fold
p=2.46e-5
HD IgAN
iv
↑1.56-fold
p=2.46e-5
HD LN
v
↑2.14-fold
p=4.97e-9
HD MN
C i
↑5.13-fold
p=0.023
Median-centered log2 CXCL1 expression
HD cFSGS
ii
↑2.69-fold
p=9.42e-4
HD DN
iii
↑1.51-fold
p=0.002
HD FSGS
iv
↑1.75-fold
p=0.002
HD IgAN
v
↑1.97-fold
p=5.32e-5
HD LN

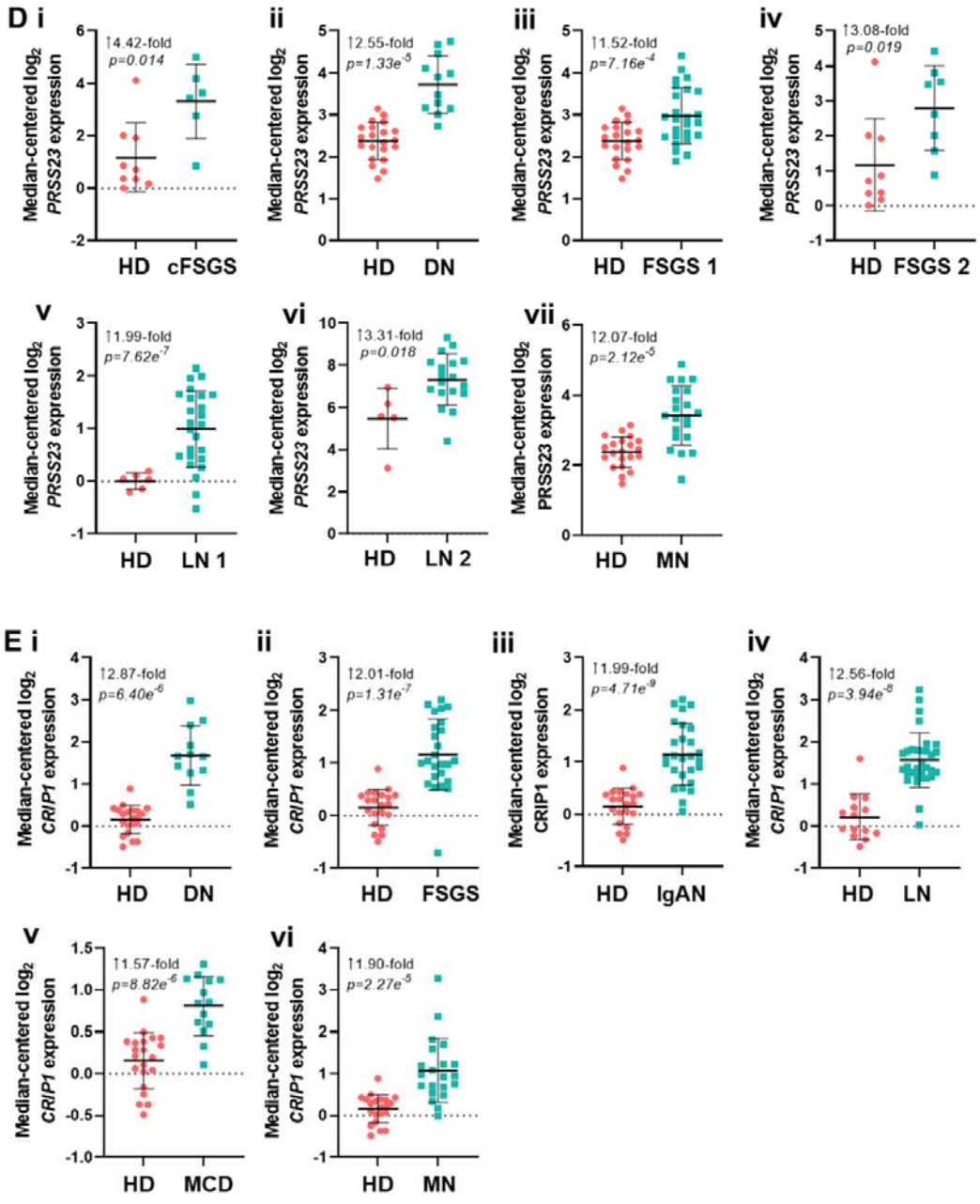
D i
Median-centered log2 PRSS23 expression
↑4.42-fold
p=0.014
HD
cFSGS
ii
↑2.55-fold
p=1.33e-5
HD
DN
iii
↑1.52-fold
p=7.16e-4
HD
FSGS 1
iv
↑3.08-fold
p=0.019
HD
FSGS 2
v
↑1.99-fold
p=7.62e-7
HD
LN 1
vi
↑3.31-fold
p=0.018
HD
LN 2
vii
↑2.07-fold
p=2.12e-5
PRSS23 expression
HD
MN
E i
Median-centered log2 CRIP1 expression
↑2.87-fold
p=6.40e-6
HD
DN
ii
↑2.01-fold
p=1.31e-7
HD
FSGS
iii
↑1.99-fold
p=4.71e-9
CRIP1 expression
HD
IgAN
iv
↑2.56-fold
p=3.94e-8
HD
LN
v
↑1.57-fold
p=8.82e-6
HD
MCD
vi
↑1.90-fold
p=2.27e-5
HD
MN

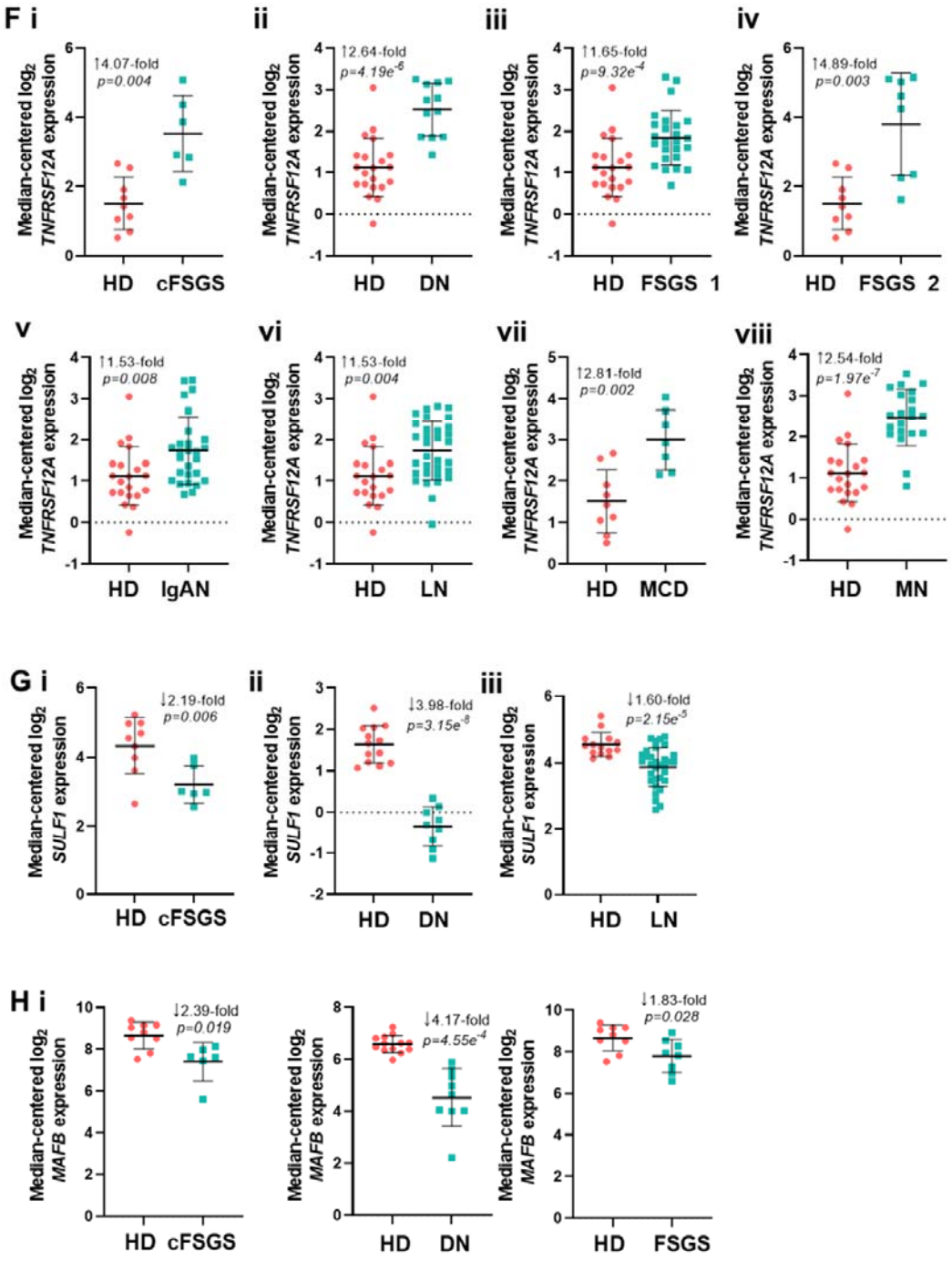


**Figure S4. Dysregulated genes shown by individual sample for each human glomerular pathology (source Nephroseq)**. Fold-change and *p* value indicated on each graph. Abbreviations as follows: HD, healthy donor; cFSGS, collapsing focal segmental glomerulosclerosis glomeruli; DN, diabetic nephropathy glomeruli; FSGS, focal segmental glomerulosclerosis glomeruli; IgAN, IgA nephropathy glomeruli; LN, lupus nephritis glomeruli; MCD, minimal change disease glomeruli; MN, membranous nephropathy glomeruli.

**Supplementary Tables S1, S2 are provided as separate Excel files.**

| Disease model | Up or downregulated | No of genes | Classified in GO:0002376 – *immune system process* |
|---|---|---|---|
| WT1 glomerulopathy (*Wt1*$^{R394W/+}$) | Upregulated | 3 unique (5) | ***Tmem178***, ***Prdx2,*** *Cxcl1, Cd59b,* ***Tcim*** |
| | Downregulated | 10 unique (14) | ***B2m***, *Zbtb20, Vegfa, Ctsh,* ***Tnfsf13***, ***Il34***, ***Bcl6***, ***Stat1***, ***H2-D1***, *H2-Q6,* ***H2-Q4***, ***H2-K1***, ***H2-T23***, ***Cd59a*** |
| Glomerulonephritis (nephrotoxic nephritis) | Upregulated | 12 unique (24) | *Cxcl2, Cd74, Cxcl13,* ***Ly96***, *Cxcl1,* ***Cxcl10***, ***Defb1***, ***Umod***, *Axl, Plvap,* ***Tmem176b***, ***Bst2***, ***H2-Eb1***, ***Mapkapk2***, *Lgals9,* ***Wfdc2***, ***H2-Ab1***, ***H2-Aa***, *Lgals3,* ***Ppp1r14b***, *Relb, Nfkb2,* ***Slamf9***, *Anxa1* |
| | Downregulated | 2 unique (7) | *Ifitm2, Zbtb20, Vegfa,* ***H2-Q7***, ***Prdx1***, *Ctsl, H2-Q6* |
| Diabetic nephropathy (BTBR *Lep*$^{ob/ob}$) | Upregulated | 18 unique (12) | ***Gm8909***, ***Akirin1***, ***Vegfd***, ***H2-Q10***, *Cxcl1,* ***Gata3***, *Axl, Plvap,* ***H2-DMb2***, *Lgals3,* ***Slpi***, ***Slc39a10*** |
| | Downregulated | 1 unique (7) | *Ifitm2, Zbtb20, Vegfa, Ctsh, Ctsl, H2-Q6,* ***Tir7*** |
| Congenital FSGS (*Cd2ap*$^{-/-}$) | Upregulated | 2 unique (11) | ***B2m***, *Cd74, Cxcl13, Cxcl1, Cd59b, Axl,* ***H2-D1***, *Lgals9, Relb,* |
| | Downregulated | 1 unique (1) | ***Ackr3*** |

**Table S3. Podocyte differentially expressed genes classified in 'GO:0002376 - *immune system process'* across murine glomerular scRNA-seq datasets.** Podocyte differentially expressed genes from murine scRNA-seq datasets of *Wt1*$^{R394W/+}$, nephrotoxic nephritis, *Lep*$^{ob/ob}$ diabetes and *Cd2ap*$^{-/-}$ that are classified into the broadest immunological GO term: *GO:0002376 – immune system process.* Genes unique to each disease model are in bold, the total number of differentially expressed genes classified is in parentheses.